2D DYNAMIC MESH MODEL FOR DEPOSIT SHAPE PREDICTION IN BOILER BANK OF RECOVERY BOILER WITH DIFFERENT TUBE SPACING ARRANGEMENTS

García Pérez, M.* and Vakkilainen, E.
*Author for correspondence
Department of Energy Technology,
Lappeenranta University of Technology,
Lappeenranta, P.O. box 20, 53851,
Finland,
E-mail: manuel.garcia.perez@lut.fi

ABSTRACT

CFD tools are essential in the design and operation of boilers. One particular aspect that can be modelled by CFD is the deposition and plugging in heat transfer surfaces of boilers. Fouling and slagging are the most typical causes of unscheduled boiler shutdowns. This is why appropriate predictions of deposition geometries and rates are of high interest. Among other applications, CFD Multiphase approaches are capable of modelling particle-laden streams. However, the relatively large number of models to select, each one with its own properties, typical applications, benefits and drawbacks- creates difficulties when trying to determine which model to use at first approach.

The problem that we are going to tackle is of a really complicated and multidisciplinary nature (thermo-fluid mechanics, sticking/rebounding of particles, sintering, among others). Dynamic mesh capabilities in commercial CFD software packages are able to modify the interphase fluid-deposit according to the growth rate, assuming it has been accurately calculated by a convenient multiphase model for particle-laden flows. In this work, such a CFD model for prediction of deposition shapes in a classical boiler bank of a Kraft Recovery Boiler will be developed and presented. The effect of tube transversal spacing will also be analyzed.

INTRODUCTION

Since their invention in 1934, recovery boilers have improved the pulp and paper mill industry. As a part of the Kraft pulping process, they allow the recovery of inorganic cooking compounds which are necessary for fiber extraction process and further cyclical reutilization. They also provide the necessary process energy by generating steam for the mill. However, since the fuel –black liquor– is not typical and since there exist two main desired outputs (energy and smelt) from the boiler, their operation, modelling and design are usually more difficult than in any other boiler application [1]. In addition, the fact that black liquor is a very ashy fuel makes the performance of Kraft Recovery Boilers (KRBs) a big challenge.

Broad research is being carried out at present when talking about modelling of boilers of any type. CFD provides us with a powerful tool to numerically solve the complex Navier-Stokes partial differential equations. When used properly, these CFD approaches can predict adequately the effects of almost any fluid-involving problems. Furthermore, they constitute a really powerful asset for designing processes. Phenomena present in boilers (fluid motion, turbulence, heat transfer, chemical reactions and combustion, transport of mass/particles, agglomeration, deposition, fouling, erosion, and pollutant and emission formation) are intended to be solved by this style of modelling [2-4].

NOMENCLATURE

$\vec{a_t}$	[m^2]	Area vector of face i
c_P	[J/kgºC]	Gas Specific heat
D	[m]	Tube diameter
$[F]$	[kg/ m^3]	Fume concentration
k	[W/mºC]	Thermal conductivity
$L_\perp$	[m⊥]	Unit of length perpendicular to a 2D model
m	[kg]	Deposited mass
N	[-]	Number of periods to simulate in a cycle
p	[Pa]	Pressure
$\vec{r}$	[m]	Node displacement vector
S_i	[m^2]	Surface generated in face I after displacement $\vec{r}$
s_t	[m]	Spacing transverse
t	[min]	Length of a cycle simulation
T	[ºC]	Temperature
T	[s]	Length of period of vortex shedding
u_∞	[m/s]	Flow velocity

Special characters

ε	[-]	Deposit porosity
η	[-]	Heat transfer performance
θ	[rad]	Angular coordinate for tube
μ	[kg/m·s]	Fluid viscosity
ρ	[kg/m^3]	Density

Figure 1: Deposit plug in a KRB shutdown between the boiler bank and the boiler bank screen. Deposits on the leading edge were close to plug the whole space between them.
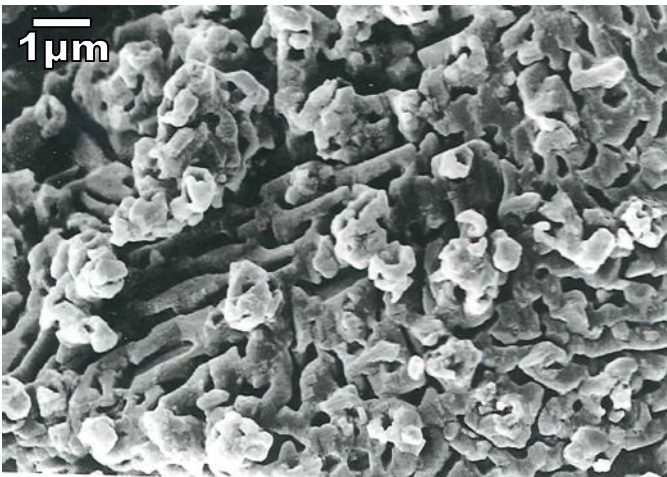
Figure 2: Micrograph of fume retrieved at an Electrostatic Precipitator of an eastern Finland KRB

A tool that can model accurately all the phenomena present in a boiler is not possible yet due to the fact that this is a multidisciplinary problem which entails really complex formulations, and also because the domain (i.e., the region that we are trying to model) can itself be of high complexity. Even with a narrow scope it may happen that a particular problem is still hard to handle, e.g., an analysis of chemistry should take into account many reactions among different phases of reactants, including phase changes. This is why CFD approaches often try to model a specific part of the boiler and solve an aspect of the phenomena. Modelling requires that some accuracy has to be lost by means of simplifying hypothesis, among which the most inevitable one is usually the fact that the mesh being used is reliable and capable of predicting accurately the target of the study.

In [2], Weber *et al.* analyzed the state of the art about CFD usage for ash behavior prediction. In their work, it is highlighted that there is not a broad usage of these tools for boiler operations. In fact, many of their results are still considered merely indicative. It was noticed that little work has been done on models that include accurately the effect of flow patterns over tube arrays. It will be shown later that the mesh needs to match specific resolution requirements in order to predict the particle motion effectively. It was also highlighted that there is no much work done on models that consider carefully the flow over tube arrays, and that also the models often do not execute a transient study of the case, losing the effects of Von Karman vortex shedding and Coanda effect. These effects lead to a swinging fashion in the motion of the flow over tube arrays [3].

The model presented here will simulate and calculate fume deposition on tubes of a boiler bank of a KRB by means of dynamic meshes. Special care will be taken at resolving the flow pattern accurately around a tube array consisting of periodical repetitions in the transversal spacing of a row of 6 tubes. In order to illustrate the effect of different flow patterns, different transversal tube spacing will be simulated. A discrete phase model shall be used to simulate the ash particles in the flow. The deposition rate in the tube surfaces will be computed, and the deposit subdomain will grow accordingly.

Case study

Due to the amount of particles and the relatively narrow tube spacing in the boiler banks, they constitute a critical point (Figure 1) regarding deposit issues [1, 4]. This work will present CFD simulations of the fume deposit growth in heat transfer surfaces of boilers.

The effect of different transversal tube spacing s_t will be studied. In their study, Nishikawa *et al.* [3] analyzed flow patterns over arrays of tubes. They found that the flow patterns do not experience important modifications from longitudinal spacing varying from 2 to 4 times the tube diameter D. However, in this range, there exists an important pattern change as s_t varies across $2 \cdot D$. This research will focus on that transition and show the flow patterns and their effect of fume depositions of tubes.

A parametric analysis on the s_t, with 6 different simulations, will be carried out. Every case will present a computational domain consisting of a row of 4 pipes, with a typical boiler bank tube diameter of D=50mm. Spacing longitudinal shall be $3 \cdot D$=150mm between the centers of the pipes. Translational periodic boundary conditions on the sides of the domain ensure an array configuration. Symmetry boundary conditions should not be applied since the flow pattern is not symmetrical although the geometry is.

The width of the domain shall be different in each case, ensuring a pipe array treatment. The parametric analysis of the transversal spacing will consist of 8 different cases, varying the spacing from 1.25 to 8 times the diameters, in steps of $0.25 \cdot D$.

Special care will be taken of resolving accurately the flow pattern. A discrete phase model shall be used to simulate the ash particles in the flow. The deposition rate in the tube surfaces will be computed, and the deposit subdomain will grow accordingly by means of a dynamic mesh update. Important care on transient considerations will be highlighted.

Ansys FLUENT enhanced with user-defined functions is used in this work.

MODEL DESCRIPTION
Discrete phase model

A Lagrangian approach is going to be used for the track of particles. This kind of model (also called the Discrete Phase Model) solves firstly the main phase (gas) alone and then models the dilute phase (particulate) by means of a certain number of discrete injections, considering each particle (or parcel of particles) separately. It is possible then to detach the particulate phase influence from the continuous phase, or consider coupling among phase calculations. This latter option would imply that, after the calculation of the particulate trajectories takes place, the continuous media is modified accordingly to recalculate afterwards new particle trajectories again; in an iterative process. This model has been proved to work well for flows where the volume fraction of particles is below 10%. A higher volume fraction would lead to a too strong coupling between the dilute phase (gas) motion and the particle phase motion.

Tomeczek *et al*. [5] created a model for shape prediction in Fluent. Even though they performed a steady state model, they showed that the mass can be computed with the macro DEFINE_DPM_EROSION. In this model, that function was coded to add up every mass flow due to particles which reach a wall face.

Fume stream motion

For the simulations, a carryover-free stream will be assumed. Carryover in a recovery boiler is a major component of the deposit. Due to inertial impaction, the windward edges of the leading tubes in heat transfer tube banks are prone to carryover deposits. The actual flow is not free of carryover; however, this model focuses on fume deposition, which tends to be somewhat more uniform within the surfaces.

Since fume is to be analyzed, special considerations must be taken. Very small particles' motion is significantly affected by flow drag. Therefore, inertial impaction (i.e., impaction due to the flow being unable to carry the particle as it detaches from its original path to surround an obstacle) is not expected for fume. On the other hand, thermophoresis and Brownian motion constitute the major mechanism of deposition for submicron particles [1, 4]. These two phenomena shall be considered in this model by enabling their respective options in the software package.

Transient considerations

The combination of Karman vortex streets and Coanda effect leads to a periodically unsteady flow in the wake of the tubes. When tubes are arranged in different manners, different patterns of flow are shed. Some of these patterns are prone to deposition of small-sized particles in the leeward part of the tube due to vortexes and swinging of the main flow direction [3]. This justifies the need for a careful transient consideration of the problem. Several CFD models for deposition of particle fail to consider a careful transient treatment of the problem [2, 5]. Figure 8, in the Results section, demonstrates this effect.

The velocity field is shown after 48 min (6 cycles of 8 min) of simulated deposit growth between 1st and 2nd tubes, with $s_t = 1.75 \cdot D$. It would be impossible to catch such a pattern with a transient simulation, as can be seen in other approaches.

It is known that for CFD simulations of flow past tube or tube arrays, the simulated frequency of vortex shedding depends on the time step used for transient consideration. There exists a step small enough below which the frequency is time-step independent. It should be fine enough, compared to the real vortex frequency. There exist some good articles which propose reliable calculations of vortex shedding for single-pipe flows. However, those correlations failed to predict accurately an appropriate vortex shedding period for tube arrays. Therefore, care should be taken, and a small enough time step needs to be selected. It will be assumed here that a time-step of 0.1ms is good enough.

Due to computing time reasons and to the very small time-step selected, it is not possible to run a calculation over a whole sootblowing rest (hours) of actual flow-time with that time step. However, in order to obtain statistically reliable data, it is necessary that long enough simulations are performed before considering updating the mesh.

Therefore, the model will proceed as follows: Firstly, the flow is simulated with particles until vortex shedding is stable. Then, the period of vortex shedding, T, is measured. Once T is known, a simulation over N periods of flow will compute the fume deposition rate in every tube face (in kg/s). The result of this will be used to calculate the total mass deposited over a whole *cycle*. Here, a *cycle* is defined as the real-time resolution (not simulated flow-time) of mesh updating. The length of the cycle will be specific for each simulation. It will be considered here that a number of N=10 will present a reasonable compromise between statistically robust data and computational time requirements.

In other words, the total mass deposited during a period of time of $10 \cdot T$ will be used to compute the mass deposited during the total cycle t_{cycle}:

$$m_{cycle} = m_{simulation} \frac{t_{cycle}}{N \cdot T} \qquad (1)$$

After simulating the flow during N periods, this m_{cycle} will be computed, and the mesh will be updated accordingly. Each mesh update accounts for the deposited mass in that cycle only, which is reset to 0 each time.

Ideally, calculations over many whole periods of flow time, in order to obtain a better and statistically robust result, would be simulated. However, this approach is not reasonable in terms of computation time. For this model, the flow with particles is initialized and let run until the vortex shedding becomes quasi stable and the domain shows no regions free of particles. The period of vortex shedding is measured, and calculations go on over 10 periods, computing at the same time the total amount of mass deposited at the tube surfaces.

INTRINSIC CFD FEATURES
Two-dimensional flow

Deposition and other phenomena involved, such as turbulence, are three dimensional mechanisms. However, due

to computing limitations and the fact that the geometry presents adequate features, this model will assume a 2D crossflow over pipes motion.

Because of this, numeric results obtained by the model will be per unit of length perpendicular to the domain. Some input and output parameters will be divided by the perpendicular to flow length unit, in this work denoted as $L_\perp$.

Mesh

A study [6] stated that many CFD models fail to predict accurately fine particle deposition on tube surfaces due to poor mesh quality. Concretely, models with poor meshes were tested and showed a tendency to overestimate inertial impaction in small particles. Coarse meshes may have good performance for big particles such as carryover, but for fume particles, fine meshes are required. Simulations were made to find out that the particle impaction efficiency seemed to become grid-independent when 380 nodes (or more) are placed in the circumference of the pipes for all kinds of particles.

As discussed earlier, the diameter of the tubes was D=50mm. It was assumed that the computational domain should start from 4·D upstream the leading edge of the first tube and span until 7·D beyond the lee edge of the last tube. The height of the domain spans accordingly to the considered s_t (different in each simulation).

Due to dynamic mesh requirements which shall be discussed later, triangular cells are required, and an initial deposit zones have to exist in each tube. Therefore, the tubes were surrounded initially with a deposit layer of 0.1mm. The tubes and the interfaces deposit-flow were meshed with 380 nodes. Triangular mesh was created in each deposit. For the flow cell-zone, a mesh size function was set up to control the cell growth as a function of the distance from the pipes. A growing factor of 1.2 was set, starting from size 0.25mm allowing a maximum cell size of 2.5mm. The final mesh was as shown in Figure 3.
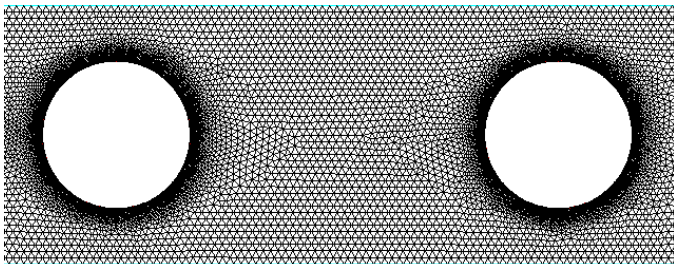
Figure 3 Mesh for s_t=1.75·D. Figure focuses on the space between 2nd and 3rd tube.

Dynamic Mesh, requirements

As commented earlier, a dynamic mesh model will be used to modify the deposit layer in each tube, according to the computed mass; by moving the deposit-flow interface. In order to avoid overlapping and extremely skewed elements in the process, the so-called "smoothing" and "remeshing" methods are applied [7].

Spring-based smoothing method treats the grid as a network of interconnected springs. Therefore, the moving interface can be seen as a wall which is pushing the nodes

away, and the displacement is shared and absorbed by several nodes layers away from the interface. Thus, nodes can re-locate and accommodate in order to preserve minimum mesh quality; overall close to the boundary. The damping of the network is controlled by a parameter called spring constant factor: a value close to zero means almost no damping, therefore, a displacement of a zone will affect cells far away; on the other hand, a value close to one will mean that the movement is completely absorbed by the closest cells.

In spite of the usage of spring smoothing methods, an excessive accumulated displacement of the interface will eventually lead to very coarse cells in the deposit and very small cells in the fluid. In order to avoid this, a local-face remeshing algorithm collapses cells the size of which is below a certain threshold into bigger ones; and reversely, it breaks or divides large cells into smaller ones. This process also helps reducing the skewness of cells. The major disadvantage of a local-face remeshing is that it is only implemented for triangular (tetrahedral in 3D) cells. Hence, quadrilateral cells are not possible here. This is why pure triangular paved schemes have been used to mesh the model.

For our simulation, a spring constant factor of 0 was selected to prevent the boundary layer close to the interface from deforming excessively. In addition, this helps preventing negative-volume cell formation. For remeshing thresholds, the minimum cell size allowed was 0.4mm, whereas the maximum cell size was 3mm.

Face-node interface update

Whereas the mass deposition is a parameter collected in the faces of the interphases, the growth of the deposit is driven by displacing the nodes in it. The determination of the displacement of every node on the deposit interface is not evident. For a better understanding, consider Figure 4 in which the update of the position of node j is defined by the vector $\vec{r}$ (in red) which needs to be determined. For a better view, the angle between faces has been exaggerated. In the real simulation, faces are quasi parallel, due to the fine discretization of the pipe.
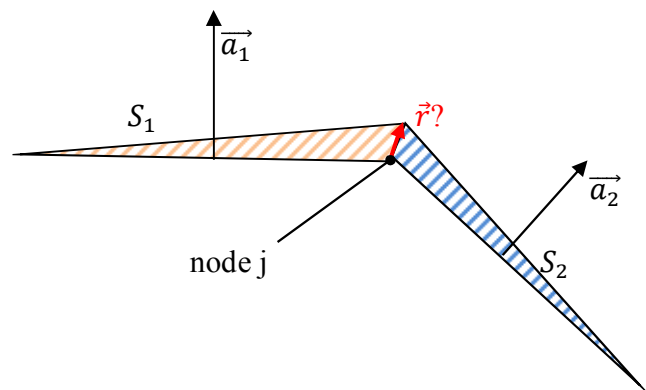
Figure 4 Detail of the update of a node j.

Vectors $\vec{a_i}$ represent the area vectors of each face, pointing outside of the pipe (towards the direction of the growth). The displacement $\vec{r}$ (red vector) will lead to an increase of the deposit. The increase of the deposit due to the movement of

node j is equal to the sum of the surfaces of the shaded triangles, i.e., $S_1 + S_2$. The desired surface of each triangle can be determined as:

$$S_i = \frac{1}{2}\frac{m_i}{\rho_{dep}} \qquad (2)$$

In (2), m_i is the mass that the model computes for the face (extrapolated to the whole cycle) and ρ_{dep} is the density of the deposit. The factor m/ρ_{dep} represents the growth, in m, that the face should have. The factor ½ has been introduced to share the effect of the deposited mass in the face between the two nodes around it. Another point of view of this factor can be explained by the fact that the displacement of one node should be obtained by averaging the growth of the surrounding faces. This value of S_i has units of surface as computed by the previous expression since the deposited mass is given in $kg/m_\perp$.

These surfaces can be computed since we know the deposit in each face. Ideally (later a problem will appear with this method), we can derive these surfaces in terms of $\vec{a_i}$ and $\vec{r}$ as the area of a triangle:

$$S_i = \frac{1}{2}|\vec{a_i}| \cdot \left[|\vec{r}| \cdot \cos(\widehat{\vec{r},\vec{a_i}})\right] \qquad (3)$$

Since $|\vec{a_i}|$ is the base of the triangle, and the term between square brackets is the height of the triangle, derived as the scalar projection of $\vec{r}$ over the direction of $\vec{a_i}$. Direct inspection of the latest equation yields that it is the dot product of these 2 vectors. Taking that into account and combining (3) and (2), the expression can be recast as:

$$\frac{m_i}{\rho_{dep}} = \vec{a_i} \cdot \vec{r} \qquad (4)$$

This expression constitutes a set of two (one for each face surrounding node j, i=1 and i=2) classical linear equations to determine the components of $\vec{r}$.

These equations can be solved through Cramer's rule. It should be mentioned that the solving of these equations becomes problematic when considering very fine meshes. The matrix of the equation system is composed by the vectors $\vec{a_i}$ in rows. The more nodes are set in the circumference, the more parallel adjacent faces become, and therefore, the more parallel these vectors become. It is known that the solutions of a linear equation system are linearly dependent on the inverse of the determinant of the matrix. This determinant approaches zero as the vectors of the matrix become linear dependent (i.e., parallel). Therefore, a very high resolution mesh would lead to numeric cancellation in the denominator of these quantities. Moreover, if one of the faces happens not to have deposition, then the displacement vector would be parallel to that face (not to generate any area for it); and this kind of displacement yields to very highly skewed and poor-quality cells. For these reasons, this method yielded non-stabilities, skewed elements and negative cell volumes as shown in Figure 5.

To circumvent this problem, a more stable method is required. It is possible to achieve it by fixing the direction of the vector $\vec{r}$ as the average direction given by $\vec{a_1}$ and $\vec{a_2}$. The magnitude of $\vec{r}$ should be the one that leads to a generation of area (deposit) equal to the sum $S_1 + S_2$. This proceeding does not match each generated surface separately, but the sum of both. Nevertheless, this solution does not imply important error, smoothes the displacements, and is numerically stable. The final expression for this new procedure to obtain the displacement results in:

$$\vec{r} = \frac{\vec{a_1}+\vec{a_2}}{|\vec{a_1}+\vec{a_2}|} \cdot \frac{m_1+m_2}{|\vec{a_1}|+|\vec{a_2}|} \cdot \frac{1}{\rho_{dep}} \qquad (5)$$

The first term is the computation of the unitary vector in the direction that we desire. The second factor is the average deposition density [kg/m^2]. The last term is the conversion of that density to actual displacement.

Figure 5 shows the comparison between these two approaches, for an artificial (non-simulated) smooth deposit distribution, in a mesh with a structured boundary layer. 5-(1): Detail of the mesh at initial conditions (not deformed). 5-(2): Same location as 5-(1) after 6 iterations of the first method (unstable). Notice highly skewed elements and the formation of negative cells in the deposit. 5-(3): Same location after 10 iterations with the second approach. The growth of the deposit remains stable. 5-(4): Zoom-out of the same pipe after 200 mesh update iterations. The interface is smooth, corresponding well to the deposition. Notice the work of the smoothing and remeshing methods: elements are suitable and low-skewed.

(1)   (2)

(3)   (4)
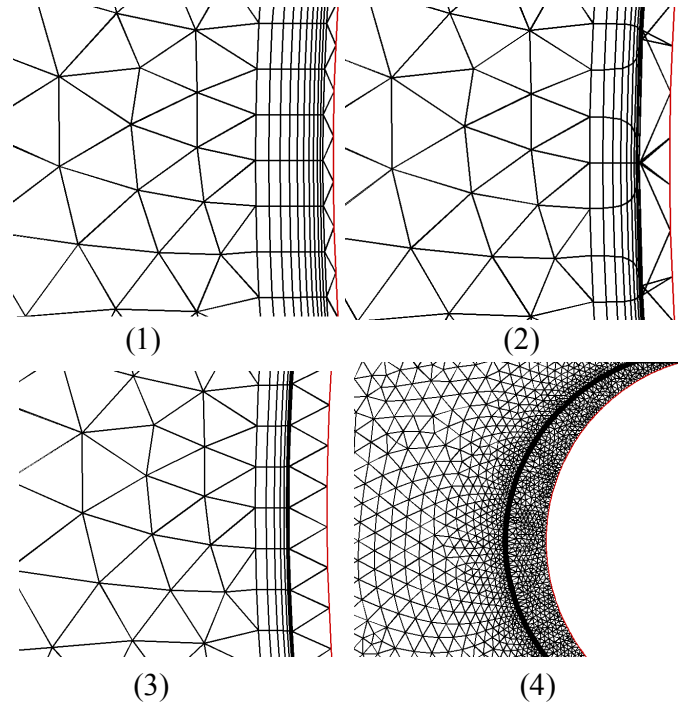
Figure 5 Different fates for different methods for updating the interface node positions.

MODEL SET-UP
Main flow conditions

Typical flow features of a classic boiler bank in KRB are required. According to [8], an incoming speed of 11.6 m/s is selected for the flow. Other selected parameters of the incoming gas flow were:

$$T = 569ºC; \quad p = 99.706 \, kPa; \quad c_p = 1.258 \frac{kJ}{kg \cdot ºC};$$

$$k = 0.0555 \frac{W}{m \cdot ºC}; \quad \mu = 3.38 \cdot 10^{-5} \frac{kg}{m \cdot s} \quad (6)$$

Due to the importance of temperature gradients, the flow needs to be considered as an ideal gas with a molecular weight of 28.13 g/mol. The temperature of the tube wall surface will be 305ºC.

The mass flow of fume must be calculated before the particle injection. It can be computed from typical values of fume concentration. A value of 6 g/m³ has been selected corresponding to actual measurements in particulate flow [9]. For a 2D model, the mass flow per unit of perpendicular length is:

$$\frac{\dot{m}_{fume}}{L_\perp} = s_t \cdot u_\infty \cdot \rho \cdot [F] \quad (7)$$

where $[F]$ denotes the fume concentration.

Properties of particles

Although particles typically follow a specific diameter distribution, a very high peak appears at $d_p = 0.7\mu m$, whereas other diameters have no significant weight. Thus, for sake of simplicity, only that constant value of particle diameter was considered here. Typically fume has a 0.95 mass fraction of sodium sulphate [1], the rest is mainly sodium carbonate and potassium sulphate. Therefore, for the model the physical properties of the particle (density, thermal conductivity and specific heat) have been taken as the ones of the sodium sulphate.

Due to the low mass and volume fraction of particles in the stream, a weak coupling between the discrete and dilute phases is expected. In a transient solution, the model tracks particles individually. The sources of the dilute phase motions will be affected by the particles only once at the beginning of each time step. There will be no particle-flow coupling recalculation within a time-step iteration.

Ash and deposition phenomena involve typically somewhat inorganic chemistry reactions among the components which are taking part. It is suggested [2] that accurate ash formation and deposits should be assessed with the help of an experienced fuel engineer/mineralogist. Some current deposition models include the effect of chemistry among ash leading substances [2, 10]. However, these phenomena fall out of the scope of this work which focusses more on the CFD proceedings and accurate flow field solving. Therefore, for sake of simplicity, inert particles will be considered here.

Stickiness of particles is a very complicated problem itself. Ideally, functions that calculate the stickiness efficiency of particles (ratio of particles that stick in a surface over the total amount of particles that hit the surface) should be included. Such a function would depend on many parameters (particle velocity, molten fraction and angle, surface properties). Concretely, temperature has a major importance: particles are not pure substances, therefore they are especially sticky within a temperature window at which the molten mass fraction spans from 15% to 70%.

T_x stands for the temperature at which a x% of the mixture is molten. Vakkilainen [11] developed a tool for ash properties

predicting in KRB. Fume corresponding to measurements was predicted to have melting temperatures of 545ºC, 777ºC and 828ºC for T_0, T_{15} and T_{70}, respectively. The temperature which is considered here is 569ºC [8], eq (6). This is below T_{15}, therefore stickiness efficiency correlations or formulae would come very handy. However, not much work has been done in this field for boiler deposition applications. Hence, in this work, a stickiness efficiency of 50% will be assumed as constant. Future research towards experimental correlations of stickiness efficiency is encouraged.

Deposits

The major feature of the deposit affecting the model is its shape, the motion updating of which has already been described.

Heat transfer losses can be accurately modelled by artificially modifying the thermal diffusivity. As the deposit expands, more material is added. It will be assumed that the characteristic time of deposit growth is very large compared to the characteristic time of transient conduction within the deposit, and also large in comparison to the simulated time (N periods, as discussed earlier). In order to avoid this, the thermal diffusivity $k_{dep}/\rho_{dep}c_{p,dep}$ must be made very large. Then, after every mesh update, the new deposit should not take many time-steps to acquire its quasi-steady temperature profile, ensuring a better reliability for the thermophoresis effect.

Since k_{dep} affects the steady temperature profile and ρ_{dep} is fixed to compute the deposit growth, a very small value for the specific heat will be artificially set to achieve our proposal.

Since the deposit is a mixture of several fume-components [1], its density shall be computed by mass-averaging those of the fume. A density of $\rho_{fume} = 2600 kg/m^3$ has been computed for this purpose. Is should be noticed that it is very close to the density of the major fume component, Na_2SO_4.

These deposits are not compact. Since they are made out of deposited particles, it will present a certain porosity. This porosity eventually reduces as a consequence of sintering [11]. Volume shrinkage and hardening of deposit will be the target of a future study; however, they fall out of the scope of the present one. It is necessary to account for porosity in the deposit since the real deposit density has to be smaller than that of the fume. It is straight-forward to deduce that, given the porosity ε, the deposit will show an "effective" bulk density of $\rho_{dep} = \rho_{fume}\varepsilon$. In this model, a constant porosity of 0.5 will be assumed.

Turbulence

Reynolds number based on the tube diameter and upstream velocity is 6867, falling in the turbulent regime. Even though the upstream velocity may not be as representative as it usually is in flow past a row of pipes, fully developed turbulent flow is ensured since velocities can be only higher surrounding the tubes (due to the fact that the array configuration leads to a significant reduction of the cross area for the flow). Since the accuracy is critical in near-wall regions, a SST k-ω model has been selected with standard input.

For the boundary conditions, a turbulent intensity of 7% and a value of 10 for the viscosity ratio were assumed.

Flow-particulate interaction

Stoke's drag law is typically suggested for tracking of very small particles. A Cunningham correction factor of 5.49 has been computed following the instructions and formulae in [7].

This model does not account for buoyancy effects.

RESULTS AND DISCUSSION

Results for simulations at spacing transverse of 1.25 and 1.75 times the diameter will be presented here. The rest of cases will be shown in the conference with more detail to the trends.

Simulation ID (s_t/D)	$\dot{m}_{fume}$ [g/s·m⊥]	T [ms]	Cycle [min]
1.25	14.5	12.00	4
1.75	20.3	13.02	8

A coordinate to describe the position in a pipe will be needed. The angle θ for each tube is defined as shown in Figure 6:

Flow direction

Figure 6 Definition of coordinate θ.

The length of each cycle simulation was decided after running the first 10 periods of flow. The length of the cycle was adjusted to obtain moderate growths ($\approx 0.5 mm$) in order to avoid excessive mesh deformation. However, some problems appeared with this approach which will be detailed in the following section.

Mesh problems: Negative-cell volumes and cracks

Deposit distribution had to be smoothed by spreading the mass of a hitting particle into the surrounding faces. Still, excessive peaks of deposition had to be cut in order to avoid mesh malfunction and negative-volume cell formation, as shown in Figure 7.
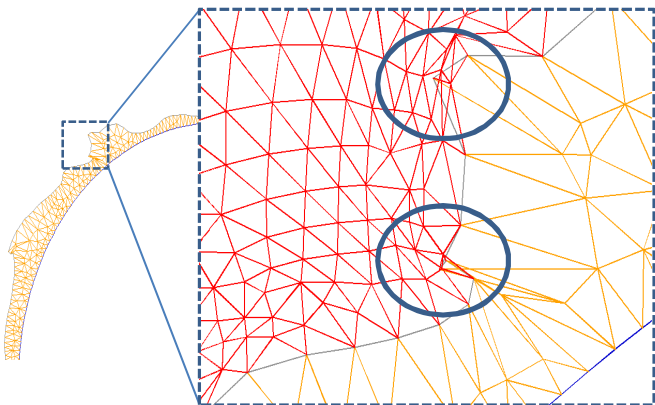
Figure 7 Negative volume formation. For the case s_t=1.25·D, second tube, in the transition from the 6th to 7th period.

Figure 7 highlights the formation of negative volumes. Cells of the flow domain (in red) have entered (overlapped) the deposit region (orange), and vice versa, resulting into negative volumes and non-possibility of continuing the calculation. Due

to strong Coanda effect, the high-velocity stream leaving the tight spacing between tubes deviates towards the opposite side of the following tube, leading to a heavy and irregular deposition in angles close to $\theta \approx \pm 3\pi/4$. Figure 8 illustrates this specific moment. There, it is shown that a strong jet impacts around $\theta = 3\pi/4$ of the second tube. As discussed, this is the place where negative volumes tend to appear.

The stream becomes faster and stronger as s_t reduces, because of the constriction of area for the gas to flow. The shape of the deposits can be appreciated.
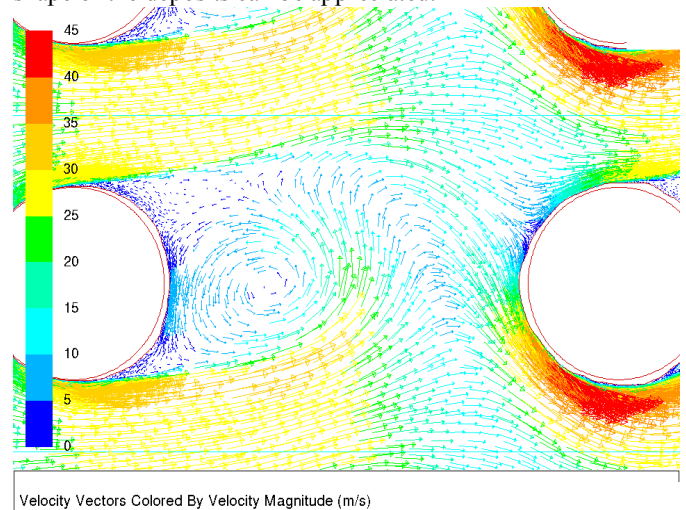
Velocity Vectors Colored By Velocity Magnitude (m/s)

Figure 8 Capture of flow field view pattern. The view is between the 1st and 2nd tube, s_t=1.75·D. Flow field captured after 56 min (7 cycles)

To avoid this problem, a procedure was set to cut the excessively high peaks of deposit. The mean value (μ) and typical deviation (σ) of the deposition was calculated, and deposits beyond a threshold of μ+2σ were cut down to that value. However, this was not enough to avoid crack formation in the limit of the threads (i.e., the first and last face of the interfaces, as they are registered in the memory of the computer), as explained in the following paragraph.

Each node position update depends on the already-done update of the preceding node, in a loop over faces procedure. Nodes are updated one by one until reaching one node which has not still been updated. Non-consistent cracks appear at the place where the loop starts and ends. This is highlighted in Figure 9. It may be possible to enable further filtering and smoothing of the deposition surface in order to avoid this. These additional techniques, which shall be included in future work, are out of the scope of this paper. In this work, cracks were manually corrected in order to be able to continue the simulation.

Deposition mass

Figures 10 and 11 are sets of graphs of the aggregated accumulated mass. Each color ribbon represents the mass added in each cycle simulation. The growth can be assumed to have a similar shape to the deposited mass.

A clear deposition close to the leading edge of each pipe (θ=π) can be appreciated. However, in both cases, it can be seen that the first tube presents less this kind of deposition than the
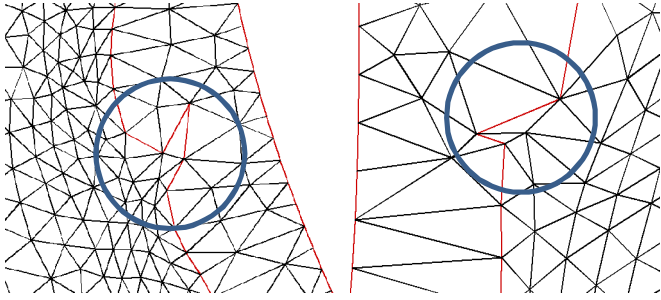
Figure 9 Cracks appearing at the points where the loop takes place. Further iterations on the mesh according to eq. (5) would eventually lead to the collapsing of interfaces and generation of non-positive cell volumes.

other tubes; supporting the hypothesis that inertial impaction is not the major mechanism of deposition for fine particles. Very little amount of mass has been deposited on the sides of the tubes ($\theta=\pi/2$ and $\theta=3\pi/2$), mainly due to the high speed of the flow tangential to the tubes. The particles do not have time to travel towards the tube crossing the boundary layer in this area. This effect was stronger at smaller spacing transverse due to the constriction of cross area.

The first tube presents generally a smaller amount of deposition than the other ones. The rest of the tubes present a somewhat similar mass deposition. Also, the first tube distribution is different from the other tubes. This is product of the flow pattern, as the flow reaches the first tube in a different way (turbulent-uniform flow) from which it reaches the following ones (vortexes and unsteady swinging jets, as in Figure 8). An increasing spacing transverse seems to lead to

higher depositions on the lee side of the first pipe, in areas close to $\theta=\pm\pi/4$.

An increase on the spacing transverse resulted into a general reduction of the total deposited mass (per pipe). This was the main reason why different lengths of cycle simulation needed to be selected for each case individually.

These graphs highlight the presence of peaks and the source of mesh problems as cycle iterations are performed. Further smoothing and filtering of mass distribution is necessary to perform a high number of cycle iterations leading to a considerable deposit growth. With appropriate mass distribution treatment, it could be possible to simulate even until sootblowing limits.

Heat transfer penalty

Being porous and insulating material, the thermal conductivity of the deposit is very low. Then, the deposit growth coats the tubes and supposes a penalty in heat transfer. For this work, a value of 0.08 W/m·K ·was chosen. This conductivity is deliberately low, but still within typical range [13]. Figure 12 shows the temperature field for the case $s_t/D=1.25$. The temperature gradient is practically concentrated within the deposit, and therefore, the gas does not cool down as it could at the initial conditions. It is possible to evaluate the performance by computing the total temperature drop of the flue gas within the domain (T_{inlet}- T_{outlet}). This temperature difference will reduce as deposit growths. Relative heat performance is defined here as:

$$\eta(t) = \frac{T_{inlet}-\overline{T_{outlet}}(t)}{T_{inlet}-\overline{T_{outlet}}(0)} \qquad (8)$$
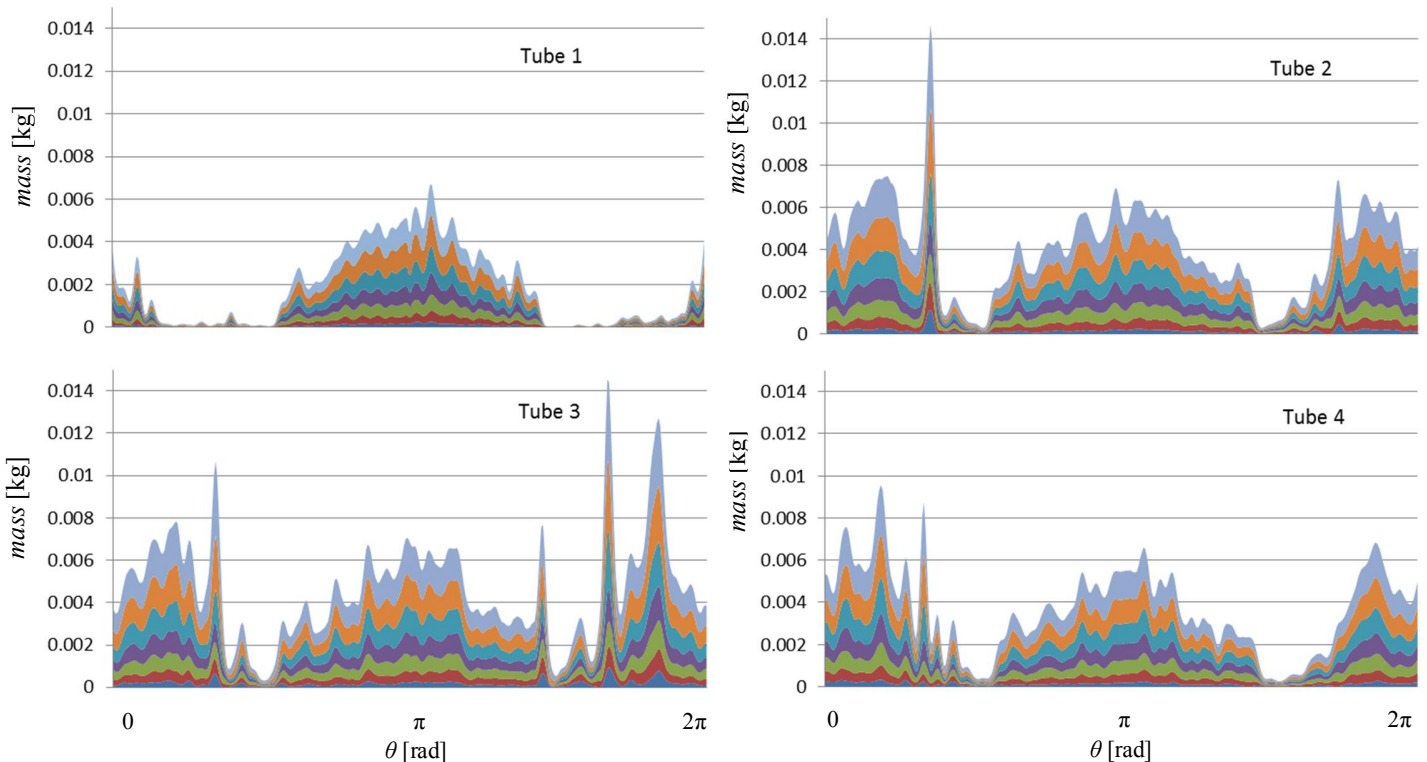
Figure 10 Deposited mass for $s_t/D=1.25$ The use of simple smoothing functions as described before was still not enough to ensure smooth and peak-free mass distribution. Apparently, peaks trend to amplify themselves from cycle to cycle, leading to eventual mesh problems described earlier.
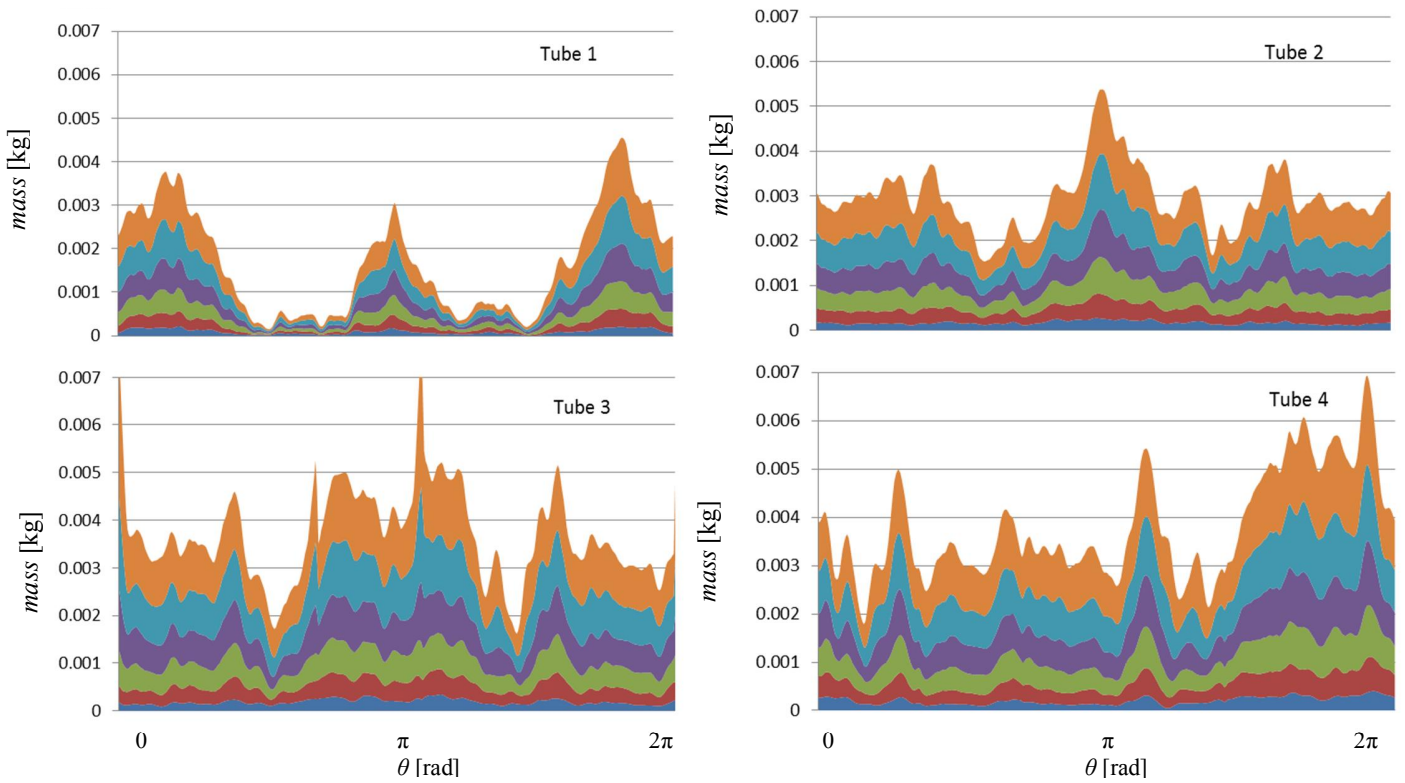
Figure 11 Deposited mass for $s_t/D=1.75$
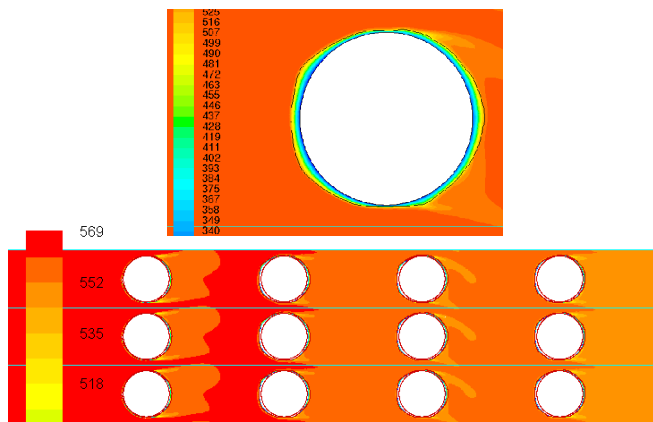
Figure 12 Temperature field. High temperature gradient in the deposit is highlighted.

T_{inlet} is constant and uniform (569ºC), but the temperature at the outlet must be integrated and area-averaged (length-averaged in this 2D model) as:

$$\overline{T_{outlet}} = \left[\int_0^{s_t} T_{outlet}(y)dy\right]/s_t \qquad (9)$$

The results are summed up in Figure 13. Already in 40 min, the performance dropped to 50%. This model reduced drastically before 50% compared to a clean pipe. Actual values measured in a KRB would not be this low because the conductivity is typically somewhat higher than the one selected

here. Moreover, as an actual deposit sinters and porosity decreases, conductivity would reach moderately higher values.

This penalty seems to be more problematic with smaller s_t. The decrease in the performance becomes smaller with the time. Coating becomes less effective as the deposit growth. Also, thermophoresis becomes less important as the temperature of the deposit surfaces increases and approaches the flow temperature; thus, the decreasing of deposition rates with time was expected.
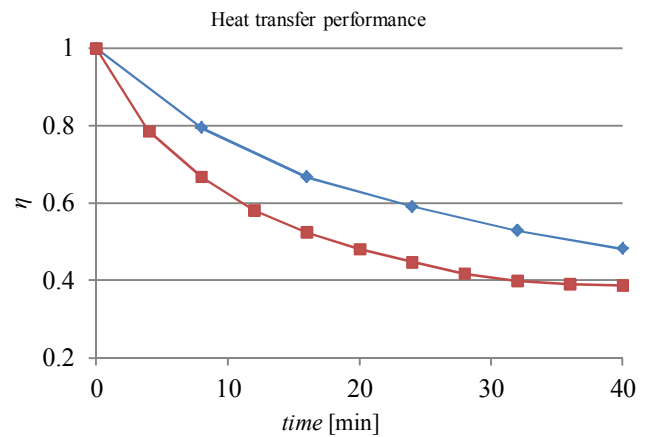
Figure 13 Heat transfer performance drop during time of deposit growth. ◆ 1.75D ■ 1.25D

CONCLUSIONS

In this work, a CFD model for prediction of deposition of ash in tube banks of a Kraft Recovery Boiler was presented. A commercial CFD package was used (FLUENT) with user defined function for the calculation of the deposited mass. A Lagrangian approach was used to track the ash particles. A single particle diameter and one Reynolds number was used. The transverse pitch ratio of the bundle was varied. The flow analysis is two-dimensional and transient, and captures vortex shedding in the wake of the tubes. Periodic boundary conditions were used in the transverse direction.

An innovative feature of the study is the dynamic mesh adaption to the shape of the interface between the gas phase and the ash deposited on a tube surface.

Difficulties with the dynamic mesh generation were illustrated and discussed. Sample results of the mass deposition profile around some tubes were presented.

Little work has been done on this field with special care about the transient fluid flow pattern. It has been highlighted that models for prediction of deposition should not consider steady-state flows, as typically can be found in literature.

The model demonstrated that the tube arrangement has a major influence in the deposition, due to vortexes formation in the lee side of the tubes. The model analyzed the important penalty on heat transfer capability due to deposit growth. It was shown that larger transversal spacings seem to show smaller depositions, and therefore smaller penalties on heat transfer performance.

There is not a lot of work done on modelling moving deposition interfaces by using dynamic meshes. This approach seems to be a powerful potential tool, still to be developed, for fouling prediction. However, appropriate smoothing algorithms on the mass distribution are necessary to avoid negative-volume cell formation and cracks. Simple smoothing approaches were attempted. This made it possible to run several cycles; however, high-skewed and non-positive elements tend to appear eventually. Thus, enhanced smoothing-filtering methods for the mass distribution could improve the model.

In order to develop the model, some assumptions had to be made. Some of these assumptions were reasonable and do not carry much error. However, not having included carryover in the model requires that the deposition rates might have to be corrected, at least for the leading edges of the first tubes due to inertial impaction.

Future work should be carried out for improvement. It is possible to control the variables of this deposit, even at low level. Therefore, by coding User-Defined Functions, it is possible to enhance the model with the inclusion of improved particle stickiness probability correlations, sintering and/or hardening of the deposit. Moreover, the inclusion of these phenomena along with particle chemistry consideration, and three dimensional turbulence flow simulated with LES would enhance the calculations broadly.

A similar approach could be tested with a different multiphase model. Eulerian multiphase model does not treat the particle phase as a discrete phase. On the contrary, particles are treated as continuum media along with the fluid. There is a strong coupling between the solutions of both phases they affect the source terms in the Navier-Stokes equations of each other one. Eulerian multiphase models have been proved to be reliable under a very wide range of applications, including particle-laden flows. An analysis of this model with an Eulerian approach could lead to interesting results to compare with, and another style of carrying out research in this field.

The usage of CFD tools for the deposition phenomena is still in an early stage, and their results can only be taken as orientative (observation of trends). However, the capabilities of this sort of tools seem to be only potentially limited by computing resources, which are expanding constantly. A lot of research is necessary (and is being carried out) in order to expand this state of the art and produce CFD models with reliable results.

REFERENCES

[1] Adams T, Frederick J, Grace T, Hupa M, Lisa K, Jones A. Kraft recovery Boilers. Atlanta, GA, USA: Tappi Press; 1997. ISBN: 0-9625985-9-3.

[2] Weber R., Mancini M., Schaffel-Mancini N., Kupka T. On predicting the ash behaviour using Computational Fluid Dynamics. *Fuel Process Technology* 2013 1;105(0):113-128.

[3] Ishigai S, Akagawa K, Fujii T, Nakanishi S, Nishikawa E, Ozawa M. Steam Power Engineering: Thermal and Hydraulic Design principles. Cambridge University Press, 1999. ISBN: 0-521-62635-8.

[4] Vakkilainen, E. Kraft Recovery Boilers – Principles and Practice. Suomen Soodakattilayhdistys r.y. Valopaino Oy. Helsinki, Finland. 2005. ISBN 952-91-8603-7.

[5] Tomeczek J, Wacławiak K. Two-dimensional modelling of deposits formation on platen superheaters in pulverized coal boilers. *Fuel* 2009 8;88(8):1466-1471.

[6] Weber R, Schaffel-Mancini N, Mancini M, Kupka T. On Importance of Fluid Dynamics in CFD Predictions of Ash Deposits. *Proceedings of the 1st Impacts of Fuel Quality on Power Production and the Environment Conference*; 2012 Sept 23-27; Puchberg Austria.

[7] Ansys FLUENT: Ansys FLUENT 14.0 User's Manual; November 2011.

[8] Vakkilainen, E. Offdesign Operation of Kraft Recovery Boiler [dissertation]. Lappeenranta University of Technology, Finland; 1992.

[9] Jokiniemi J, Pyykönen J, Mikkanen P, Kauppinen E. Modeling fume formation and deposition in kraft recovery boilers. *Tappi Journal*, vol. 79 no.7, pp 171-181.

[10] Pyykönen J, Jokiniemi J. Modelling alkali chloride superheater deposition and its implications. *Fuel Processing Technology*, Volume 80, Issue 3, 15 March 2003, Pages 225-262, ISSN 0378-3820. http://dx.doi.org/10.1016/S0378-3820(02)00240-0.

[11] Vakkilainen, E. Predicting Ash Properties in Recovery Boilers. *Proceedings of the 2010 International Chemical Recovery Conference*, March 29 - April 1, 2010, Williamsburg Lodge, Williamsburg, Virginia, USA, Vol. 2, pp. 237 – 245. 2010.

[12] Frederick, W.J.; Vakkilainen, E.K.; Tran, H.N.; Lien, S.N. The Conditions for Boiler Bank Plugging by Submicrometer Sodium Salt (Fume) Particles in Kraft Recovery Boilers. *Institute of Paper Science and Technology (IPST)* at Georgia Institute of Technology, 500 10th Street NW, Atlanta, Georgia 30332-0620. February, 2004.

[13] Baxter, Larry L., 1998, Influence of ash deposit chemistry and structure on physical and transport properties. *Fuel Processing Technology*, Vol. 56, No. 1-2, July 1998, pp. 81 - 88.